



## P-binding mineral materials to enhance phosphate removal using nature-based solutions in urban areas

Agnieszka Bus\*, Agnieszka Karczmarczyk

*Department of Environmental Development, Warsaw University of Life Sciences - SGGW, Nowoursynowska 166, 02-787 Warsaw, Poland, Tel. +48 22 59 35 099; email: agnieszka\_bus@sggw.edu.pl (A. Bus), Tel. +48 22 59 35 382; email: agnieszka\_karczmarczyk@sggw.edu.pl (A. Karczmarczyk)*

Received 9 January 2020; Accepted 10 July 2020

---

### ABSTRACT

The increase in urbanization has caused a deterioration of the quality of water bodies and ecosystems such as rivers, streams and lakes. Urban hydrology, which reflects the anthropogenic impact on water balance, results in an excess of phosphorus (P) and their eutrophication in urban water bodies. Nature-based solutions (NBS) are a measure for the restorations of green areas and the mitigation of urban stormwater problems. Despite many advantages, in some specific cases (e.g., green roofs), NBS may be a source of water pollution. The way to decrease P release from NBS construction is by using P-binding mineral materials (P-BMM). The aim of the study is: (1) to assess the sorption abilities of five different P-BMMs: autoclaved aerated concrete (AAC), Filtralite® Nature P (FNP) (Norway), limestone, Opoka and zeolite, (2) to determinate of the equilibrium contact time with P solution, and (3) to dimension the P-BMM filter mass needed to enhance P-removal from green roof run-off before it reaches the receiver. Based on the Langmuir isotherm equation, P-BMM maximum sorption capacity ( $S_{max}$ ) and equilibrium sorption capacity ( $S_{max,Eq}$ ) follow the sequence: FNP > Opoka > AAC > zeolite > limestone. The most suitable P-BMM for filling up the filter for green roof runoff seems to be AAC. This is because it took the shortest time to achieve equilibrium (300 min) and had high  $S_{max,Eq}$  value (66.28 mg g<sup>-1</sup>). The mass of AAC P-BMM needed to provide the P retention from 100 m<sup>2</sup> of a green roof ranges from 2.4 to 11.2 kg. The P-BMM filter, with a discharge to rain garden, was proposed as a P-removal enhancing system for green roof runoff.

*Keywords:* Green roof; Phosphorus; Reactive materials; Urban environment; Water harvesting

---

### 1. Introduction

Cities are becoming a living environment for an increasing number of people. Roughly more than 72% of the total EU-28 population lives in cities, towns and suburbs [1] and it is estimated to reach more than 80% by 2050 [2]. Globally, cities are major socioeconomic entities where more than 50% of the global population lives and where the population is forecast to double by 2050. This will pose a range of challenges for the natural resources and ecosystems,

including the rivers, streams and lakes which are a part of the landscape of many cities.

Phosphorus (P) in the environment is often related to agricultural areas and to untreated sewage. However, P in the surface water is increasingly coming from urbanized areas with sealed surfaces that generate significant surface runoff. Urban ecosystems are known to be P-rich environments where P originates from pet waste, fertilizers, grass litter, soil microbial communities, vegetative detritus and soil particles [3–5].

---

\* Corresponding author.

In this regard, nature-based solutions (NBS) are the solutions for suitable P-removal from urban water bodies given limited space. NBS are solutions based on nature that have many functions simultaneously. The most important functions are: rainwater harvesting, storing and purification, regulating air temperature and softening the urban heat island effect [6]. NBS facilitate the efficient use of natural resources and respect human well-being. They promote socially inclusive green growth by replicating the natural processes and integrating ecosystem services into the human environment [6,7].

Urban areas rainwater harvesting is often based on systems of green roofs. The leachate receivers are usually in the form of water retention ponds, constructed wetlands, bio-retention basins, rain gardens, bioswales, etc. All the NBS are used to support rainwater management and purification, overgrowing with vegetation adapted to variable water conditions. Such small freshwater ecosystems play a significant role in biogeochemical cycles due to their global abundance and their high rate of biological activity. In addition, they tend to be hotspots of contaminations (suspended soils, sediments, biodegradable organics, nutrients, heavy metals and hazardous substances, dissolved organic carbon, etc.) [5,8,9]. The choice of NBS water receiver depends mainly on the availability of space, soil and water conditions, the system functions, the need to amount of precipitation and snowmelt, solution durability, operational requirements and costs [10].

However, it must be remembered that constructions such as green roofs are often a source of P. The P concentrations from green roof runoff may vary from 0.003 mg P-PO<sub>4</sub> dm<sup>-3</sup> [11] to above 1.0 mg P-PO<sub>4</sub> dm<sup>-3</sup> [12–14]. The factors influencing the P runoff from green roofs are green roof type (intensive or extensive), amount of rainfall, local pollution sources, type and age of substrate, plants, physical and chemical properties of pollutants, fertilization and maintenance practice, and local air quality [15]. In all types of NBS, P accumulation is rather low, but it should not be considered as the main treatment target [8,16]. For example, in the case of stormwater ponds, despite the high removal efficiency of suspended solids, the P-removal rate is variable, low or even lacking [8,17,18]. For this reason, the implementation of phosphorus-binding mineral material (P-BMM) at such systems seems to be essential for keeping P concentration under control.

P-BMMs consisting of metals oxides or hydroxides have been the most successful for the uptake of different oxyanions from water. P-binding materials should be synthesized from various metals, such as Al, Ca, Ce, Fe, La, Mg, Zn and Zr. Among the rare earth elements, lanthanum and cerium have been used to remove phosphorus due to their high sorption capacity and more reasonable cost compared to other elements [19,20]. The excess P may be removed from water by various treatment processes such as physiochemical methods, biological treatment processes, ion exchange, electro-coagulation and sorption. Of these methods, sorption is most often used due to low initial cost, flexibility, and simplicity of design, and ease of operation and maintenance [21].

The aim of the study is: (1) to assess the sorption ability of five different P-BMMs; (2) to determine the

equilibrium contact time of P-BMMs with P solution and (3) to dimension the P-BMM filter mass as an additional step to enhance P-removal from green roof run-off.

## 2. Materials and methods

### 2.1. P-binding mineral materials

Five different P-BMM were used in this study: autoclaved aerated concrete (AAC), Filtralite® Nature P (FNP) (Norway), limestone, Opoka and zeolite. AAC is a lightweight popular material used in civil engineering. Quartz sand, lime or cement and water are used as binding agents. Filtralite® Nature P (Norway) is a high-quality filter media, manufactured from expanded clay material heated over 1,000°C. It is used for filtration and purification with an active surface of dolomite added for P-binding. However, dolomite enrichment is not listed in the basic composition of the material (Table 1) ([www.filtralite.com](http://www.filtralite.com)). Limestone is a sedimentary rock, composed mainly of the skeletal fragments of marine organisms. Calcined Opoka calcium silicate sedimentary rock, heated at a temperature of 900°C. Zeolite is a hydrated aluminosilicate mineral that contains alkali and alkaline earth metals. The mineral composition and scanning electron microscopy (SEM) microphotographs of the P-BMMs are shown in Table 1 and Fig. 1, respectively. The physical properties of RMs were determined in accordance with the following standards: particle size distribution PN EN 933-1:2012 and PN-ISO 11277:2005, bulk density PN EN 1097-3:2000, porosity PN-EN 1936:2010 and water absorption PN EN 1097-6:2013-11. The physical properties of the tested P-BMMs are presented in Table 2.

### 2.2. Batch tests

Different concentration of the artificial P solution prepared using KH<sub>2</sub>PO<sub>4</sub>, were used in all batch tests for assessing P sorption. The triplicate samples of material were mixed in Erlenmeyer glass flasks, each contained 1.0 g of material and 100 mL of the various P solutions. The kinetic tests were performed at various contact times (5–2,880 min) and at a constant average solution concentration of 4.5 mg P-PO<sub>4</sub> dm<sup>-3</sup>. The sorption equilibrium tests were performed at various solution concentrations (1–1,000 mg P-PO<sub>4</sub> dm<sup>-3</sup>) and for a constant time (24 h). The calculation of the P-removal ratio *R* (%) was based on Eq. (1):

$$R[\%] = \frac{C_0 - C_e}{C_0} \times 100\% \quad (1)$$

where *C*<sub>0</sub> and *C*<sub>*s*</sub> are the initial and equilibrium P concentration (mg L<sup>-1</sup>).

The sorption capacity (*q*<sub>*e*</sub>) was calculated from Eq. (2):

$$q_e = \frac{(C_0 - C_e) \times V}{m} \quad (2)$$

where *q*<sub>*e*</sub> is the sorption capacity (mg g<sup>-1</sup>); *V* is the volume of solution (dm<sup>3</sup>); *m* is the mass of material (g), and *C*<sub>0</sub> and *C*<sub>*s*</sub> are the initial and final (equilibrium) concentrations (mg dm<sup>-3</sup>).

Table 1  
Main mineral compounds of tested P-BMMs (%)

AAC
SiO <sub>2</sub> – 57.24; CaO – 24.62; Al <sub>2</sub> O <sub>3</sub> – 1.96; SO <sub>3</sub> – 1.35; Fe <sub>2</sub> O <sub>3</sub> – 1.03; MgO – 0.52; K <sub>2</sub> O – 0.48
FNP <sup>a</sup>
SiO <sub>2</sub> – 63.00; Al <sub>2</sub> O <sub>3</sub> – 17.00; CaO – 2.00; Fe <sub>2</sub> O <sub>3</sub> – 7.00; Na <sub>2</sub> O – 2.00; K <sub>2</sub> O – 4.00
Limestone
CaO – 29.30; MgO – 6.79; SiO <sub>2</sub> – 0.61; P <sub>2</sub> O <sub>5</sub> – 0.31; Fe – 0.14; Cl – 0.10
Opoka
SiO <sub>2</sub> – 55.11; CaO – 23.86; Al <sub>2</sub> O <sub>3</sub> – 5.65; Fe <sub>2</sub> O <sub>3</sub> – 2.10; K <sub>2</sub> O – 1.04
Zeolite
SiO <sub>2</sub> – 47.80; Al <sub>2</sub> O <sub>3</sub> – 6.07; CaO – 2.84; K <sub>2</sub> O – 2.19; Fe – 1.07; P <sub>2</sub> O <sub>5</sub> – 0.18; Ti – 0.14

<sup>a</sup>Producent information; Filtralite® Nature P (Norway) is enriched with natural dolomite (<https://filtralite.com/en/node/104>).

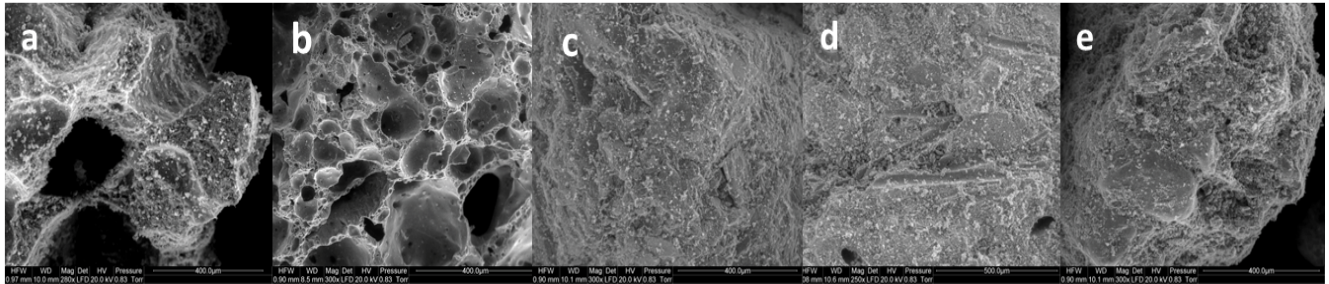


Fig. 1. Scanning electron microscopy (SEM) micrographs of (a) AAC, (b) FNP, (c) Opoka, (d) limestone and (e) zeolite (all enlarged to 400 µm).

Description of the sorption process between solid phase and solution was made based on mathematical equations given by Langmuir Eq. (3) [22]:

$$\frac{1}{q_s} = \frac{1}{C_s} \cdot \frac{1}{K_L} + \frac{a_L}{K_L} \quad (3)$$

where  $K_L$  is a constant parameter reflecting the solute adsorptivity ( $\text{dm}^3 \text{g}^{-1}$ ),  $a_L$  is a constant parameter related to the energy of adsorption ( $\text{dm}^3 \text{mg}^{-1}$ ), the  $K_L/a_L$  ratio is defined as an adsorption capacity,  $q_s$  is sorption ( $\text{mg g}^{-1}$ ),  $C_s$  is the solute concentration at equilibrium ( $\text{mg dm}^{-3}$ ), and Freundlich equation [22]:

$$\log q_s = b_F \times \log C_s + \log a_F \quad (4)$$

where  $a_F$  is a constant which expresses the adsorbent capacity ( $\text{dm}^3 \text{g}^{-1}$ ) (the larger the value, the higher the capacity),  $b_F$  is the heterogeneity factor (-),  $q_s$  is sorption ( $\text{mg g}^{-1}$ ),  $C_s$  is the solute concentration at equilibrium ( $\text{mg dm}^{-3}$ ).

The obtained results from kinetic batch experiments were fitted to two of the most widely used non-linear kinetic models: the pseudo-first-order (PFO) kinetic model (Eq. (5)) and the pseudo-second-order (PSO) kinetic model (Eq. (6)) [23]:

$$\log(q_e - q_t) = \log q_e - kt \quad (5)$$

$$\frac{1}{q_t} = \frac{1}{q_e^2 k_2} + \frac{t}{q_e} \quad (6)$$

where  $q_t$  ( $\text{mg g}^{-1}$ ) represents the amount adsorbed at any time  $t$ ,  $k_1$  ( $\text{min}^{-1}$ ) and  $k_2$  ( $\text{g mg}^{-1} \text{min}^{-1}$ ) are rates of sorption of the PFO and PSO and  $q_e$  is the amount adsorbed at equilibrium ( $\text{mg g}^{-1}$ ).

The P equilibrium concentrations were measured by flow injection analyses using FIAstar 5000 at the ranges of (0.005–1.000  $\text{mg P-PO}_4 \text{ dm}^{-3}$ ) and (0.500–5.000  $\text{mg P-PO}_4 \text{ dm}^{-3}$ ). All samples were filtered by a syringe filter of 0.45 µm pore size.

### 2.3. Dimensioning of the P-BMM filter

The data for the dimensioning of P-BMMs were taken from a previous study [24] with columns filled with five different intensives (3) and extensive (2) green roof substrates collected from a local market (Table 3). The experiment lasted 90 d and during this time 470 mm of tap water was supplied to each column which corresponds to the amount of rainfall observed in the vegetation season in central Poland. For the dimensioning of the P-BMM filter, a load of  $\text{P-PO}_4$  leached out from each substrate was used.

Table 2  
Physical properties of tested P-BMMs

	AAC	FNP <sup>a</sup>	Limestone	Opoka	Zeolite
Grain size (mm)	2–6	0.5–4.0	1–2	2–6	1–2
pH (–)	9.0	≈12.0	8.8	10.8	8.5
Porosity (%)	83.7	60.0	40.0	38.0	50.0
Bulk density (g cm <sup>-3</sup> )	0.30	0.37	1.50	0.78	0.90
Water adsorption (%)	70.0	60.0	4.0	5.3	9.0

<sup>a</sup>Producent information (<https://filtralite.com/en/node/104>).

Further calculations were performed for the green roof with an area of 100 m<sup>2</sup> and a thickness of 0.2 m. The thickness value corresponds to substrate thickness recommended both for intensive and extensive roofs [25].

The dimensioning of P-BMM mass followed the steps:

- Conversion of the P-PO<sub>4</sub> unit load to a roof with an assumed area (100 m<sup>2</sup>) and substrate thickness (0.2 m) base on the bulk density.
- Calculation of the equilibrium sorption capacity ( $S_{\max\_Eq}$ ) base on  $S_{\max}$  value and P-PO<sub>4</sub> reduction in equilibrium time.
- Estimation of P-BMM filters mass (kg) base on P-PO<sub>4</sub> load (i) and  $S_{\max\_Eq}$  value (ii) according to Eq. (7):

$$M_{P-BMM} = \frac{Y \cdot L}{S_{\max\_Eq}} \quad (7)$$

where  $Y$  is the number of years of operation (year),  $L$  is the seasonal load of P-PO<sub>4</sub> (g y<sup>-1</sup>) and  $S_{\max\_Eq}$  is an equilibrium sorption capacity (g kg<sup>-1</sup>).

### 3. Results and discussion

#### 3.1. Kinetic studies

The PFO and PSO kinetic studies are important in order to evaluate the mechanism and efficiency of the sorption process. Adsorption kinetics expresses the physical and/or chemical nature of adsorption interaction dependence of the P-BMM with phosphates. Sorption dynamics of the tested mineral materials as a function of time were fitted to the PFO and PSO kinetic models to obtain the data presented in Fig. 2. The most rapid P-PO<sub>4</sub> removal is seen with Opoka and AAC. After 5 min of contact time 32% and 16% of P-PO<sub>4</sub>, respectively was removed from the solution. After 5 min of contact time, other tested P-BMM after 5 min of contact time removed between 1%–2% of P-PO<sub>4</sub>. However, none of the tested P-BMMs removed 100% of P-PO<sub>4</sub> after 4,880 min. The best results were 96%, 90% and 89% for AAC, FNP and Opoka, respectively. The equilibrium was reached the fastest with AAC (300 min). Opoka, limestone and zeolite needed 720 min and FNP as long as 1,440 min. This statement is confirmed by the  $k$  value (Table 4) which follow the sequence: AAC > Opoka > limestone > zeolite > FNP. The parameters of PFO and PSO are set out in Table 4. Based on the calculations (Table 4), the removal of phosphates onto tested P-BMMs follows the PSO kinetic

models. The reaction described by the PSO kinetic model suggests that chemisorption is the rate-limiting step [26–28]. Riahi et al. [28] speculated that the adsorption of phosphate species can be reasonably presumed to occur in the following steps: transfer of phosphate from the aqueous solution to the sites on the P-BMM and chemical complexation or ion exchange at the active sites and precipitation on the P-BMM surface. It is well known that the process of phosphate uptake onto tested P-BMMs appears to occur over three stages as observed Zhang et al. [29]: (1) a first sharper reaction stage which is clearly seen during the first minute of contact time, (2) a low reaction stage at 60–300 min, and (3) at equilibrium stage with strong and stable adsorption (Fig. 2).

#### 3.2. Isotherm studies

The two most common isotherm models (Langmuir and Freundlich) were used to investigate and describe the removal process between phosphate solution and solid phase. The Langmuir isotherm model assumes a completely homogenous surface where the sorption onto the surface has the same activation energy. The Freundlich isotherm model, however, is suitable for highly heterogeneous surfaces [30]. It is noted from  $R^2$  values that adsorption isotherms of phosphate in tested P-BMMs could be described by both the Langmuir and the Freundlich isotherm models. However, the Langmuir model fits better for all tested P-BMMs ( $R^2 > 95.75\%$ ) and the coefficients for the plots were higher than those obtained using the Freundlich model (Table 5).  $S_{\max}$  and  $K_F$  factor in Langmuir and Freundlich isotherm models are usually used to evaluate the adsorption capacity of phosphate. The higher obtained values implied a larger phosphate adsorption capacity of the tested P-BMMs [31]. In all tested P-BMMs the adsorption reactions follow the Langmuir isotherm model. According to Chen et al. [21] and Guo et al. [31], good compliance with the Langmuir model suggests that phosphate adsorption is mainly controlled by the chemisorption process. This statement is confirmed by kinetics studies.

Maximum sorption capacity values ( $S_{\max}$ ) calculated according to the Langmuir isotherm parameters are set out in Table 6. The values ranged from 4.95 to 116.28 mg g<sup>-1</sup>. Than the  $S_{\max}$  sequence follows: FNP > Opoka > AAC > zeolite > limestone. Then, the values of  $S_{\max}$  were reduced by phosphate reduction noted at equilibrium. In this way, the equilibrium sorption capacities  $S_{\max\_Eq}$  were recalculated for the reduction rate at equilibrium that equaled: 0.93, 0.89, 0.72, 0.82 and 0.72 for AAC, FNP, limestone, Opoka and

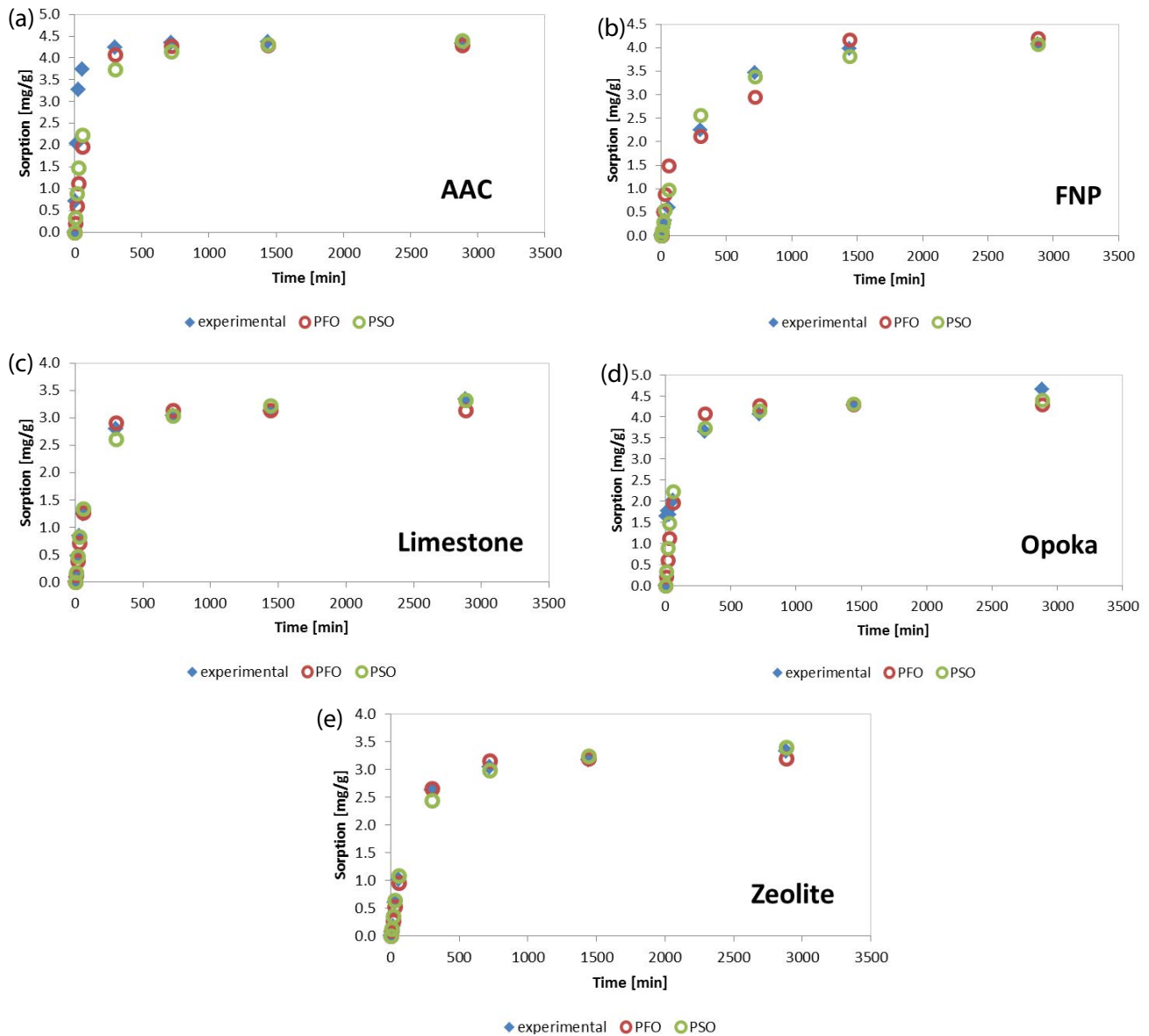


Fig. 2. Effect of contact time of the experimental data and results of PFO and PSO for tested P-BMM (a) AAC, (b) FNP, (c) limestone, (d) Opoka and (e) zeolite.

Table 3

Data from column leaching experiment [24]. Column area 0.144 m<sup>2</sup>; substrate thickness 0.04 m

Substrate	S1	S2	S3	S4	S5
Type	Intensive	Intensive	Intensive	Extensive	Extensive
Composition	mineral-organic	mineral-organic	mineral-organic	no data	mineral
Bulk density (kg m <sup>-3</sup> )	1,054.8	1,051.1	983.4	1,145.6	1,498.7
Precipitation (mm)	470				
Volume of leachate (mm)	330.7	308.3	323.9	308.8	346.5
Mean leachate P-PO <sub>4</sub> concentration (mg dm <sup>-3</sup> )	0.116	0.242	0.286	0.050	0.060
Unit load of P-PO <sub>4</sub> (kg m <sup>-3</sup> )	0.908	1.773	2.351	0.337	0.346

Table 4  
Calculated parameters of the pseudo-first and pseudo-second-kinetic order

P-BMM	Pseudo-first-order model			Pseudo-second-order model		
	$k_1$ (min <sup>-1</sup> )	$q_e$ (mg g <sup>-1</sup> )	$R^2$ (%)	$k_2$ (g mg <sup>-1</sup> min <sup>-1</sup> )	$q_e$ (mg g <sup>-1</sup> )	$R^2$ (%)
AAC	0.04394	4.1994	99.48	0.06426	4.4760	99.65
FNP	0.00266	4.0735	97.36	0.00475	4.3759	97.88
Limestone	0.00864	3.1407	99.73	0.01064	3.4371	99.81
Opoka	0.01022	4.2875	94.64	0.01647	4.4933	95.70
Zeolite	0.00594	3.1927	99.77	0.00731	3.5509	99.95

Table 5  
Langmuir and Freundlich isotherm parameters

P-BMM	Langmuir isotherm			Freundlich isotherm		
	$K_L$ (dm <sup>3</sup> g <sup>-1</sup> )	$a_L$ (dm <sup>3</sup> mg <sup>-1</sup> )	$R^2$ (%)	$a_F$ (dm <sup>3</sup> g <sup>-1</sup> )	$b_F$ (-)	$R^2$ (%)
AAC	0.6129	0.0086	99.98	0.6073	0.2893	93.90
FNP	126.11	1.0836	97.70	0.8454	3.9121	93.76
Limestone	0.6624	0.1337	96.20	0.4186	0.1760	83.88
Opoka	41.549	0.4144	98.47	0.6229	2.0996	73.33
Zeolite	0.7095	0.1200	98.75	0.4189	0.1160	83.01

Table 6  
Maximum sorption capacity  $S_{\max}$  and equilibrium sorption capacity  $S_{\max,Eq}$  (mg g<sup>-1</sup>) for tested P-BMMs

	AAC	FNP	Limestone	Opoka	Zeolite
$S_{\max}$	71.27	116.28	4.95	100.26	5.91
$S_{\max,Eq}$	66.28	103.49	3.56	82.21	4.26

zeolite, respectively. The  $S_{\max,Eq}$  values are lower than the  $S_{\max}$  values of 7%, 11%, 28%, 18% and 28% for AAC, FNP, limestone, Opoka and zeolite, respectively. The results for calculated  $S_{\max}$  and  $S_{\max,Eq}$  are set out in Table 6. To the best of our knowledge, there has been no attempt to revise the  $S_{\max}$  value by reduction rate at equilibrium based on kinetic studies, but in this way, the time needed to reach equilibrium is taken into account.

### 3.3. pH vs. potential P-removal mechanism

The high pH of P-BMMs (Table 2) is a result of the release of Ca<sup>2+</sup> that occurs in all the tested materials in various contents (Table 1). P-BMMs rich in Ca<sup>2+</sup> are characterized by high pH (10–12) due to the Ca<sup>2+</sup> precipitation as CaCO<sub>3</sub> in the presence of CO<sub>2</sub> and oxygen [32,33]. Calcium carbonates and hydroxides have the ability to remove P from water. The mechanisms of P-removal are generally considered to be sorption followed by precipitation of calcium phosphates. Several forms may be formed such as calcium phosphate dihydrate (CaHPO<sub>4</sub>·2H<sub>2</sub>O), octacalcium phosphate (Ca<sub>8</sub>H<sub>2</sub>(PO<sub>4</sub>)<sub>6</sub>·5H<sub>2</sub>O) and hydroxyapatite (Ca<sub>5</sub>(PO<sub>4</sub>)<sub>3</sub>OH) [7,34,35]. What is more, their dissolution causes an increase in pH [34]. For this reason,

hydroxyapatite (HAP) is the most common Ca-P precipitate, which is normally formed at high pH values (above 10). Calcium phosphate dihydrate and octacalcium phosphate are expected at lower pH values [35]. At pH values ranged from 7 to 12, HPO<sub>4</sub><sup>2-</sup> is the dominant species, probably formed as a result of increasing pH [36]. It has been claimed that the chemical precipitation process is dominant when the pH has values above 8 [37,38]. At a pH lower than 8, the precipitation of Ca-P is likely to be an intermediate process [7]. The relationship between data obtained using the Langmuir isotherm model maximum sorption capacity and the pH of tested P-BMMs is presented in Fig. 3. High values of  $R^2$  confirm the statement that P sorption is pH-dependent.

The affinity to bind P may also be increased by the calcination process. The thermal treatment at a temperature of 900°C–1,200°C promotes the decomposition of CaCO<sub>3</sub> to CaO and also increases the pH value [39]. The calcination process and appearance of CaCO<sub>3</sub> takes place with Opoka (pH = 10.8) and also with FNP (pH ≈ 12.0), a kind of light-weight aggregate [35] enriched by dolomite. Apart from Ca, the main P-removal mechanism for FNP is precipitation to aluminum and iron oxides [40]. In the case of Opoka and possibly FNP, the most active phase responsible for P-removal is CaO. The high pH value of the material is evidence of decomposition of CaCO<sub>3</sub> to CaO. The presence of CaO is the reason that these materials are more reactive to phosphorus than, for example, limestone (pH = 8.8) and zeolite (pH = 8.5). In the case of limestone, the active phase responsible for P-removal is also dependent on the content of calcium, mainly in the form of CaCO<sub>3</sub>. The main P-removal mechanisms by limestone were suggested to be the formation of Ca-complexes and precipitation mechanisms [41]. For AAC, the P-removal mechanism includes

Table 7

Phosphorus sorption properties  $S_{\max}$  comparisons of different P-BMMs with the experimental condition: mass to solution ratio; isotherm ranges concentrations and pH

Sorption ( $\text{mg g}^{-1}$ )	P-BMM	Experimental conditions	Reference
116.28	FNP	10 g L <sup>-1</sup> ; 1–1,000 mg dm <sup>-3</sup> ; pH = 12	This study
100.26	Opoka	10 g L <sup>-1</sup> ; 1–1,000 mg dm <sup>-3</sup> ; pH = 10.8	
71.21	AAC	10 g L <sup>-1</sup> ; 1–1,000 mg dm <sup>-3</sup> ; pH = 9.0	
5.91	Zeolite	10 g L <sup>-1</sup> ; 1–1,000 mg dm <sup>-3</sup> ; pH = 8.5	
4.95	Limestone	10 g L <sup>-1</sup> ; 1–1,000 mg dm <sup>-3</sup> ; pH = 8.8	
158.7	Thermal treatment Opoka	66.7g L <sup>-1</sup> ; 5–100 mg dm <sup>-3</sup> ; pH = 11–12	[43]
107.53	Synthesized lanthanum hydroxide	2.5 g L <sup>-1</sup> ; 5–500 mg dm <sup>-3</sup> ; pH = 11.3	[46]
75.8	Waste concrete	10g L <sup>-1</sup> ; 0–1,600 mg dm <sup>-3</sup> ; pH = 11.0	[44]
72.87	Calcined eggshells	10 g L <sup>-1</sup> ; 6–978 mg dm <sup>-3</sup> ; pH = 12.5	[39]
55.56	Commercial lanthanum hydroxide	2.5 g L <sup>-1</sup> ; 5–500 mg dm <sup>-3</sup> ; pH = 9.6	[46]
38.8	Fly ash	20 g L <sup>-1</sup> ; 100–1,600 mg dm <sup>-3</sup> ; pH = 8.0	[47]
33.20	Fe–Mn binary oxide	0.2 g L <sup>-1</sup> ; 2–40 mg dm <sup>-3</sup> ; pH = 10.0	[48]
21.55	Thermal treatment aerated concrete	33 g L <sup>-1</sup> ; 10–1,200 mg dm <sup>-3</sup> ; pH = 8.3	[45]
15.99	Zeolite	1 g L <sup>-1</sup> ; 12.5–200 mg dm <sup>-3</sup> ; pH = 5.3	[49]
0.017	Light-expanded clay aggregate	100 g L <sup>-1</sup> ; 0.1–2.0 mg dm <sup>-3</sup> ; pH = 8.2	[50]

physical adsorption and crystalline precipitation. The crystalline phases present in CAAC responsible for P-removal are tobermorite ( $\text{Ca}_5\text{Si}_6\text{O}_{16}(\text{OH})_2 \cdot 4\text{H}_2\text{O}$ ), gypsum ( $\text{CaSO}_4$ ), and limestone ( $\text{CaCO}_3$ ) [37]. Zeolites are characteristically contained many oxides and have a three-dimensional structure with channels and pores. In addition, zeolites possess a high ion exchange capacity. These properties make them interesting as potential filter materials [41]. Wang et al. [42] claim that the adsorption of P onto zeolites relies on electrostatic attraction or ion-exchange.

### 3.4. Comparison of P-BMMs sorption capacities

The literature describing experiments to determine the sorption capacity of P-BMMs is rich [7,19–21,23,27–30,32–39,40,43–50]. Selected materials are listed in Table 7 from lowest to highest values of  $S_{\max}$  obtained from the Langmuir isotherm model. In addition to the  $S_{\max}$  value, the conditions for conducting the experiment are also presented, for example, the mass of material to solution ratio, ranges of P concentration and pH. The highest value of  $S_{\max}$  has thermal treated Opoka (158.7 mg g<sup>-1</sup>) [43] that is 58% higher than obtained during this study. However, the mass to solution ratio is very high compared to other materials. The higher ratio (100 g L<sup>-1</sup>) [50], does not guarantee high sorption and in this case, is limited by a low range of initial concentrations. With a different kind of aerated concrete, the tested waste concrete [44] had the sorption on a similar level to that obtained in this study. On the other hand, the thermal treatment aerated concrete [45] is characterized by a sorption 30% lower.

### 3.5. P-BMMs for enhancing NBS

Data concerning loads of phosphorus in green roof runoff for the dimensioning of P-BMM were taken from a previous study [24] (Table 3). Calculated P-PO<sub>4</sub> loads from

Table 8

Mass of P-BMMs (kg) (calculated for one vegetation season)

P-BMM	S1	S2	S3	S4	S5
AAC	0.29	0.56	0.70	0.12	0.16
FNP	0.19	0.36	0.45	0.07	0.10
Opoka	0.23	0.45	0.56	0.09	0.13
Limestone	5.38	10.47	12.99	2.17	2.91
Zeolite	4.50	8.75	10.85	1.81	2.43

a green roof with an area of 100 m<sup>2</sup> and substrate thickness of 0.2 m are within the range 7,721 to 46,239 mg P-PO<sub>4</sub>. The mass of the P-BMM filters calculated using Eq. (7) are set out in Table 8.

From tested P-BMMs, the most promising sorption results were obtained for FNP, Opoka and AAC (Table 6). Limestone and zeolite were not considered for further calculations because of their low  $S_{\max, \text{Eq}}$  values. The most suitable P-BMM for the filter seems to be AAC because of the shortest time need to achieve equilibrium (300 min) and the relatively high  $S_{\max, \text{Eq}}$  value (66.28 mg g<sup>-1</sup>). The important issue for rainwater treatment is retention time. The shorter the time needed to reach equilibrium, the more efficient is the sorption. This is a desirable factor, important in the case of rain duration and intensity [8] that influences retention time [19]. Based on the calculations (Table 8), the mass of AAC as a result of the filter exploration time was estimated. According to Fig. 4, the mass of P-BMM needed to provide the P retention for 20 y, ranged from 2.4 kg (S4) to 11.2 kg (S3). However, it should be noted that this is an estimated value and is based on the assumption that in the following seasons the outflow of phosphorus from the green roof will be the same as that based on the results from the first season. Different studies report that leaching of phosphorus may be attributed to a variety of factors,

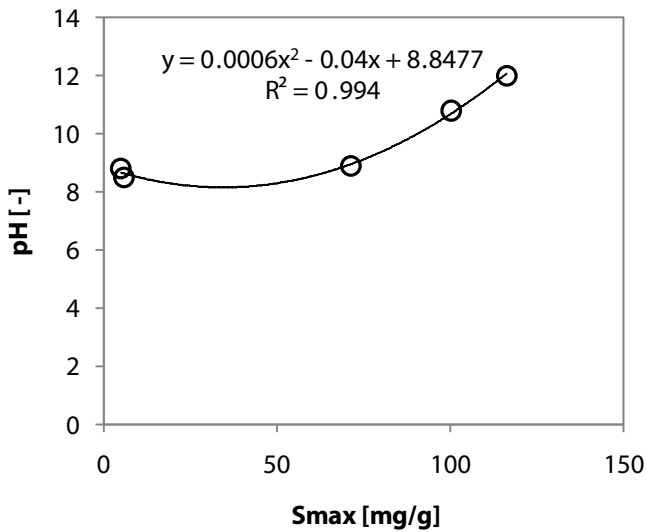


Fig. 3. The relationship between  $S_{max}$  and pH of P-BMM.

including the composition of growing media, the type and extent of vegetative cover, fertilizer use, and the age of the roof. One previous study [24] confirmed the impact of the substrate age in the case of volume-weighted mean concentrations and unit area loads, but not in the observed P-PO<sub>4</sub> concentrations range. Mitchell et al. [51] stated that roof age, followed by the summer and winter seasonal dynamics, had the greatest effect on phosphate concentrations in runoff from green roofs. There have not been enough long-term green roof studies have been carried out to clearly determine if and how long green roof will be a source of phosphorus in the runoff.

By applying the filter, it will be possible to reduce the P concentration in green roof runoff, and this could be an alternative to underlying the substrate with P-BMM layers [52]. It was found that 0.02 m of P-BMM is able to protect the water environment against P pollution. For such a solution, the considered green roof area of 100 m<sup>2</sup> should be supported by 600 kg of AAC.

The AAC was previously tested as an enhancement for the treatment of wastewater at constructed wetlands (CW) [7]. The authors mainly focused on the physical and chemical

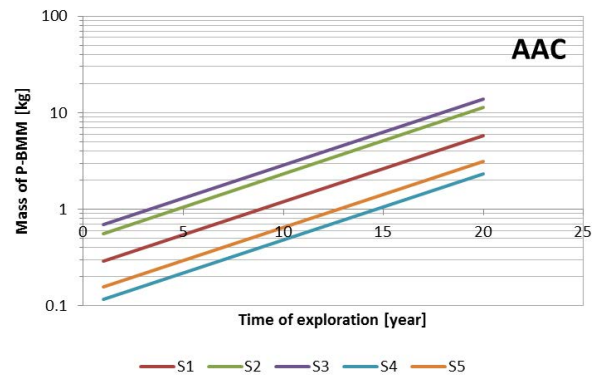


Fig. 4. P-BMM filter mass (kg) estimated for P-removal from runoff from substrates S1–S5.

Note: y-axis on a logarithmic scale.

characterization of the material to better understand the removal process in relation to the dependence of P concentration, grain size and contact time. However, there is no recommendation for practical use. Also, AAC supported the P-removal in the case of CW designed for heavily P polluted surface water [53]. The CW of 3.0 ha area should be supported by 5,000 kg AAC to reduce the P-PO<sub>4</sub> concentration to the level of 0.01 mg dm<sup>-3</sup>. Other usages of AAC as a NBS enhancement has been shown [54].

In the case considered, the runoff receiver from a green roof is a P-BMM filter. Water then infiltrates through the rain garden which is designed to retain and distribute water in the soil (Fig. 5). Rain gardens are landscape sites that reduce the flow rate, total quantity and pollutant load from urban areas [55]. The rain garden retention capacity ranges from 150 to 250 dm<sup>3</sup> m<sup>-2</sup> [10]. Assuming the average retention capacity of the rain garden of 200 dm<sup>3</sup> m<sup>-2</sup> and substrate runoff, the rain garden area is 1.65, 1.54, 1.62, 1.54 and 1.73 m<sup>2</sup> for S1, S2, S3, S4 and S5, respectively. These calculations confirm the general statement that the rain garden area should correspond to 2% of a catchment area [56]. The obtained results enable the design of a rain garden located in the native soil. A required area of 2 m<sup>2</sup> is acceptable even in that limited space of an urban environment.

In this paper, we did not discuss the treatment efficiency of the rain garden. The rain garden is only the part of the

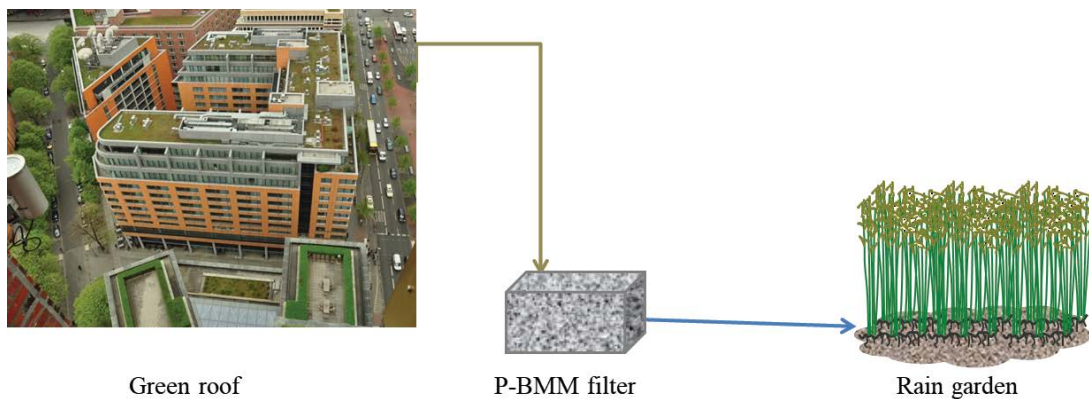


Fig. 5. NBS system enhancing P-removal by P-BMM.

system, focusing on the infiltration of the green roof and filter runoff. However, the rain garden can be also a part of the treatment system. Such constructions rely on plants and natural or engineered soil medium to retain stormwater and increase the lag time of infiltration while remediating and filtering pollutants carried by urban runoff [51]. Jiang et al. [8] rated the removal efficiency of the rain garden and bioswale with respect to total phosphorus (TP). The tested NBS were characterized by 43% and 54% of TP-removal, with initial concentrations of 0.33 and 0.42 mg L<sup>-1</sup>, for the rain garden and bioswale, respectively. The higher removal rate was a result of using a 0.2 m layer of blast furnace slag. Weiss et al. [57] compare two types of rain gardens with and without a layer of sand mixed with iron shavings at 5% w/w. In the case of iron shavings, they noted the ability to remove over 90% of dissolved phosphorus from stormwater runoff. In contrast, Dietz and Clausen [16] found that for the first year of operating the rain garden located in native soil, the retention for TP –110.6% which indicates that more phosphorus left the system than entered. AAC and other P-BMMs tested in this study could be applied as a component of the rain garden substrate to enhance the overall efficiency of system treatment. However, if implemented in a separate filter, replacement of saturated material is easy and does not interfere with the NBS construction.

#### 4. Conclusions

P-BMMs are one of the options for enhancing NBS in P-removal. Based on our results, three of the tested P-BMMs (AAC, Opoka, FNP) can be characterized by good P sorption ability from an aquatic solution that is confirmed by both  $S_{\max}$  and  $S_{\max, \text{Eq}}$  values. The P-BMM most suitable as an additional step to enhance P-removal from green roof runoff is AAC. This is because it needs the shortest time to achieve equilibrium and has a high  $S_{\max, \text{Eq}}$  value. However, it must be remembered that laboratory experiments, even those based on real substrate leakages, do not give completely representative results. Implementation should be preceded by a pilot-scale experiment.

Conceptualization, A.B. and A.K.; Methodology, A.B.; Software, A.B.; Formal Analysis, A.B.; Investigation, A.B.; Data Curation, A.B.; Writing – Original Draft Preparation, A.B.; Writing – Review & Editing, A.B.; Visualization, A.B.; Supervision, A.B, A.K.

#### Symbols

$a_L$	– Constant parameter related to the energy of adsorption
$a_F$	– Constant which expresses the adsorbent capacity
$b_F$	– Heterogeneity factor
CW	– Constructed wetland
$C_0$	– Initial P concentration
$C_s$	– Final (equilibrium) P concentration
HAP	– Hydroxyapatite
$K_L$	– Constant parameter reflects the solute adsorptivity
$k_1$	– Rate of sorption of the pseudo-first-order kinetic model

$k_2$	– Rate of sorption of the pseudo-second-order kinetic model
$L$	– Season load of phosphate
$m$	– Mass of phosphorus binding mineral material
$M_{\text{P-BMM}}$	– Phosphorus binding mineral material filters mass
NBS	– Nature-based solutions
P	– Phosphorus
P-BMM	– Phosphorus binding mineral material
PFO	– Pseudo-first-order kinetic model
PSO	– Pseudo-second-order kinetic model
$q_e$	– P amount adsorbed at equilibrium
$q_t$	– P amount adsorbed at any time $t$
$R$	– Phosphorus-removal ratio
$S_{\max}$	– Maximum sorption capacity
$S_{\max, \text{Eq}}$	– Equilibrium sorption capacity
S1–S5	– Green roof substrates from 1 to 5
$V$	– Volume of solution
$Y$	– Number of exploration years

#### References

- [1] Eurostat, Eurostat Regional Yearbook, Luxembourg, 2015. Available at: <https://ec.europa.eu/eurostat/documents/3217494/7018888/KS-HA-15-001-EN-N.pdf> (15.12.2019)
- [2] EEA, SOER – The European Environment – State and Outlook, European Environment Agency, Luxembourg, 2015. Available at: <http://www.eea.europa.eu/soer> (15.12.2019)
- [3] M.J. Paul, J.L. Meyer, Streams in the urban landscape, *Annu. Rev. Ecol. Syst.*, 32 (2001) 333–365.
- [4] K. Steinke, R.W. Kussow, J.C. Stier, Potential contributions of mature prairie and turfgrass to phosphorus in urban runoff, *J. Environ. Qual.*, 42 (2013) 1176–1184.
- [5] K. Song, M.A. Xenopoulos, J. Marsalek, P.C. Frost, The fingerprints of urban nutrients: dynamics of phosphorus speciation in water flowing through developed landscapes, *Biogeochemistry*, 125 (2015) 1–10.
- [6] European Commission, Towards an EU Research and Innovation Policy Agenda for Nature-Based Solutions and Re-Naturing Cities, Brussels. Cities, Brussels. Available at: <https://op.europa.eu/en/publication-detail/-/publication/fb117980-d5aa-46df-8edc-af367cddc202> (15.12.2019)
- [7] J.A.C. Castellar, J. Formosa, J.M. Chimenos, J. Canals, M. Bosch, J.R. Rosell, H.P. Silva, J. Morató, H. Brix, C.A. Arias, Crushed autoclaved aerated concrete (CAAC), a potential reactive filter medium for enhancing phosphorus removal in nature-based solutions—preliminary batch studies, *Water*, 11 (2019) 1442.
- [8] C.B. Jiang, J. Li, H. Li, Y.J. Li, L. Chen, Field performance of bioretention systems for runoff quantity regulation and pollutant removal, *Water Air Soil Pollut.*, 228 (2017) 468.
- [9] EEA Report No 26/2016 Rivers and Lakes in European Cities Past and Future Challenges, Luxembourg. Available at: <https://www.eea.europa.eu/publications/rivers-and-lakes-in-cities> (15.12.2019)
- [10] Katalog Dobrych Praktyk, Zasady zrównoważonego gospodarowania wodami opadowymi pochodzącymi z nawierzchni pasów drogowych, Wrocław, Poland, 2017.
- [11] B.G. Gregoire, J.C. Clausen, Effect of modular extensive green roof on stormwater runoff and water quality, *Ecol. Eng.*, 37 (2011) 963–969.
- [12] J.M. Aloisio, A.R. Tuininga, J.D. Lewis, Crop species selection effects on stormwater runoff and edible biomass in an agricultural green roof microcosm, *Ecol. Eng.*, 88 (2016) 20–27.
- [13] D.A. Beck, G.R. Johnson, G.A. Spolek, Amending greenroof soil with biochar to affect runoff water quantity and quality, *Environ. Pollut.*, 159 (2011) 2111–2118.
- [14] M. Seidl, M.-C. Gromaire, M. Saad, B. De Gouvello, Effect of substrate depth and rain-event history on the pollutant

- abatement of green roofs, *Environ. Pollut.*, 183 (2013) 195–203.
- [15] K. Vijayaraghavan, D.H.K. Reddy, Y.S. Yun, Improving the quality of runoff from green roofs through synergistic biosorption and phytoremediation techniques: a review, *Sustainable Cities Soc.*, 46 (2019) 101381.
- [16] M.E. Dietz, J.C. Clausen, A field evaluation of rain garden flow and pollutant treatment, *Water Air Soil Pollut.*, 167 (2005) 123–138.
- [17] M. O'Shea, M. Borst, C. Nietch, The role of stormwater BMPs in mitigating the effects of nutrient over enrichment in urban watershed, *Global Solut. Urban Drain.*, (2002) 1–16, doi: 10.1061/40644(2002)24.
- [18] Best Management Practice Database, International Stormwater Best Management Practices Database Pollutant Category Summary, Denver. Available at: <http://www.bm-pdatabase.org> (15.12.2019)
- [19] C. Vohla, M. Kőiv, H.J. Bavor, F. Chazarenc, Ü. Mander, Filter materials for phosphorus removal from wastewater in treatment wetlands—a review, *Ecol. Eng.*, 37 (2011) 70–89.
- [20] H. Bacelo, A.M. Pintor, S.C. Santos, R.A. Boaventura, C.M. Botelho, Performance and prospects of different adsorbents for phosphorus uptake and recovery from water, *Chem. Eng. J.*, 381 (2020) 122566.
- [21] N. Chen, W.W. Hu, C.P. Feng, Z. Zhang, Removal of phosphorus from water using scallop shell synthesized ceramic biomaterials, *Environ. Earth Sci.*, 71 (2014) 2133–2142.
- [22] G. McKay, *Use of Adsorbents for Removal Pollutants from Wastewater*, CRC Press, Boca Raton, FL, USA, 1996.
- [23] J. Lin, L. Wang, Comparison between linear and non-linear forms of pseudo-first-order and pseudo-second-order adsorption kinetic models for the removal of methylene blue by activated carbon, *Front. Environ. Sci. Eng.*, 3 (2009) 320–324.
- [24] A. Karczmarczyk, A. Bus, A. Baryła, Phosphate leaching from green roof substrates—can green roofs pollute urban water bodies?, *Water*, 10 (2018) 199.
- [25] Stowarzyszenie Wykonawców Dachów Płaskich i Fasad (DAFA). Dachy zielone. In Wytyczne do Projektowania, Wykonywania i Pielęgnacji Dachów Zielonych—Wytyczne dla Dachów Zielonych; Stowarzyszenie Wykonawców Dachów Płaskich i Fasad (DAFA), Opole, Poland, 2015.
- [26] Y.S. Ho, D. McKay, Pseudo-second-order model for sorption processes, *Process Biochem.*, 34 (1999) 451–465.
- [27] A. Bus, A. Karczmarczyk, Kinetic studies on removing phosphate from synthetic solution and river water by reactive material in a form of suspended reactive filters, *Desal. Water Treat.*, 136 (2018) 237–244.
- [28] K. Riahi, S. Chaabane, B.B. Thayer, A kinetic modeling study of phosphate adsorption onto *Phoenix dactylifera* L. date palm fibers in batch mode, *J. Saudi Chem. Soc.*, 21 (2013) 143–152.
- [29] Y. Zhang, H. Li, Y.Y. Zhang, F.J. Song, X.Q. Cao, X.J. Lyu, Y. Zhang, J. Crittenden, Statistical optimization and batch studies on adsorption of phosphate using Al-eggshell, *Adsorpt. Sci. Technol.*, 36 (2018) 999–1017.
- [30] J. Chen, Y. Cai, M.C. Clark, Y. Yu, Equilibrium and kinetic studies of phosphate removal from solution onto a hydrothermally modified oyster shell material, *PLoS One*, 8 (2013) e60243.
- [31] Z. Guo, J.H. Li, Z.B. Guo, Q.J. Guo, B. Zhu, Phosphorus removal from aqueous solution in parent and aluminum modified eggshells: thermodynamics and kinetics, adsorption mechanism, and diffusion process, *Environ. Sci. Pollut. Res. Int.*, 24 (2017) 14525–14536.
- [32] K. Adam, A.K. Søvik, T. Krogstad, Sorption of phosphorus to filterlite-PTM—the effect of different scales, *Water Res.*, 40 (2006) 1143–1154.
- [33] W.C. Tan, Q.Y. Wang, Y.B. Wang, Z.K. Pan, Adsorption of Nitrogen and Phosphorus on Natural Zeolite and its Influencing Factors, International Conference on Computer Distributed Control and Intelligent Environmental Monitoring, Changsha, China, 2011, pp. 1949–1952.
- [34] P. Loganathan, S. Vigneswaran, J. Kandasamy, N.S. Bolan, Removal and recovery of phosphate from water using sorption, *Crit. Rev. Environ. Sci. Technol.*, 44 (2014) 847–907.
- [35] R. Mliih, F. Bydalek, E. Klumpp, N. Yaghi, R. Bol, J. Wenk, Light-expanded clay aggregate (LECA) as a substrate in constructed wetlands—a review, *Ecol. Eng.*, 148 (2020) 105783.
- [36] K. Karageorgiou, M. Paschalis, G.N. Anastassakis, Removal of phosphate species from solution by adsorption onto calcite used as natural adsorbent, *J. Hazard. Mater.*, 139 (2007) 447–452.
- [37] W.J. Li, L.X. Zeng, Y. Kang, Q.Y. Zhang, J.W. Luo, X.M. Guo, A solid waste, crashed autoclaved aerated concrete, as a crystalline nucleus for the removal of low concentration of phosphate, *Desal. Water Treat.*, 57 (2016) 14169–14177.
- [38] O. Khelifi, Y. Kozuki, H. Murakami, K. Kurata, M. Nishioka, Nutrients adsorption from seawater by new porous carrier made from zeolitized fly ash and slag, *Mar. Pollut. Bull.*, 45 (2002) 311–315.
- [39] A. Bus, A. Karczmarczyk, A. Baryła, Calcined eggshell as a P reactive media filter—batch tests and column sorption experiment, *Water Air Soil Pollut.*, 230 (2019) 20.
- [40] D.J. Ballantine, C.C. Tanner, Substrate and filter materials to enhance phosphorus removal in constructed wetlands treating diffuse farm runoff: a review, *N.Z.J. Agric. Res.*, 53 (2010) 71–95.
- [41] L.J. Westholm, Substrates for phosphorus removal—potential benefits for on-site wastewater treatment?, *Water Res.*, 40 (2006) 23–36.
- [42] Y.T. Wang, Z.Q. Cai, S. Sheng, F. Pan, F.F. Chen, J. Fu, Comprehensive evaluation of substrate materials for contaminants removal in constructed wetlands, *Sci. Total Environ.*, 701 (2020) 134736.
- [43] M. Kasprzyk, M. Gajewska, Phosphorus removal by application of natural and semi-natural materials for possible recovery according to assumptions of circular economy and closed circuit of P, *Sci. Total Environ.*, 650 (2019) 249–256.
- [44] X. Liu, H.Y. Zhong, Y. Yang, L. Yuan, S. Liu, Phosphorus removal from wastewater by waste concrete: influence of P concentration and temperature on the product, *Environ. Sci. Pollut. Res.*, 27 (2020) 10766–10777.
- [45] K. Kang, C.G. Lee, J.W. Choi, S.G. Hong, S.J. Park, Application of thermally treated crushed concrete granules for the removal of phosphate: a cheap adsorbent with high adsorption capacity, *Water Air Soil Pollut.*, 228 (2017) 8.
- [46] J. Xie, Z. Wang, S.Y. Lu, D. Wu, Z.J. Zhang, H. Kong, Removal and recovery of phosphate from water by lanthanum hydroxide materials, *Chem. Eng. J.*, 254 (2014) 163–170.
- [47] M. Hermassi, C. Valderrama, N. Moreno, O. Font, X. Querol, N.H. Batis, J.L. Cortina, Fly ash as reactive sorbent for phosphate removal from treated waste water as a potential slow release fertilizer, *J. Environ. Chem. Eng.*, 5 (2017) 160–169.
- [48] G.S. Zhang, H.J. Liu, R.P. Liu, J.H. Qu, Removal of phosphate from water by a Fe–Mn binary oxide adsorbent, *J. Colloid Interface Sci.*, 335 (2009) 168–174.
- [49] J. Goscińska, M. Ptaszkowska-Koniarz, M. Frankowski, M. Franus, R. Panek, W. Franus, Removal of phosphate from water by lanthanum-modified zeolites obtained from fly ash, *J. Colloid Interface Sci.*, 513 (2018) 72–81.
- [50] J. Łożyńska, A. Bańkowska-Sobczak, Z. Popek, J.A. Dunalska, Selection of P-reactive materials for treatment of hypolimnetic water withdrawn from eutrophic lakes, *Ecohydrol. Hydrobiol.*, 20 (2020) 276–288.
- [51] M.E. Mitchell, S.F. Matter, R.D. Durtsche, I. Buffam, Elevated phosphorus: dynamics during four years of green roof development, *Urban Ecosyst.*, 20 (2017) 1121–1133.
- [52] A. Bus, A. Karczmarczyk, A. Baryła, The use of reactive material for limiting P-leaching from green roof substrate, *Water Sci. Technol.*, 73 (2016) 3027–3032.
- [53] A. Bus, A. Karczmarczyk, Supporting constructed wetlands in P-removal efficiency from surface water, *Water Sci. Technol.*, 75 (2017) 2554–2561.
- [54] A. Karczmarczyk, A. Bus, Removal of phosphorus using suspended reactive filters (SRFs)—efficiency and potential applications, *Water Sci. Technol.*, 76 (2017) 1104–1111.
- [55] Ogród deszczowy w gruncie. Instrukcja budowy. Available at: <https://sendzimir.org.pl/wp-content/uploads/2019/03/broszura-ogrod-deszczowy-w-gruncie.pdf> (10.12.2019)
- [56] EPA, Soak Up the Rain: Rain Gardens, USA. Available at: <https://www.epa.gov/soakuptherain/soak-rain-rain-gardens> (11.12.2019)
- [57] P.T. Weiss, Z.Y. Aljobeh, C. Bradford, E.A. Breitzke, An Iron-Enhanced Rain Garden for Dissolved Phosphorus Removal, World Environmental and Water Resources Congress, Florida, 2016.